

# Ultralow Surface Energy Plasma Polymer Films

S. R. Coulson, I. S. Woodward, and J. P. S. Badyal\*

Department of Chemistry, Science Laboratories, Durham University, Durham DH1 3LE U.K.

S. A. Brewer and C. Willis

DERA, Porton Down, Salisbury SP4 0JQ, U.K.

Received March 6, 2000. Revised Manuscript Received May 9, 2000

Room-temperature pulsed plasma polymerization of long-chain perfluoroacrylates produces well-adhered liquid-repellent (hydrophobic and oleophobic) films. Critical surface tension values as low as  $\gamma_c = 4.3 \text{ mN m}^{-1}$  have been measured on coated flat glass substrates. X-ray photoelectron spectroscopy, Fourier transform infrared, and atomic force microscopy characterization of these surfaces indicates that the low surface energy perfluoroalkyl chains remain intact, while polymerization occurs predominantly via the acrylate carbon-carbon double bond during the plasma duty cycle off-period.

## 1. Introduction

Hydrophobic and oleophobic repellency are highly desirable for numerous everyday applications, e.g. aerospace, lithography, sports and outdoor clothing, biomedical layers, integrated sensors, and protection against environmental fouling, etc.<sup>1-5</sup> In the case of flat substrates, it is the chemical nature of the functional group packing which governs surface wettability.<sup>7,8</sup> For instance, perfluoroalkyl chains are renowned for their liquid repellency. The tightly bound, nonbonding electron pairs surrounding each fluorine atom core shell in F-C bonds are not easily polarized, and therefore hinder hydrogen bonding and dispersion interactions with polar and nonpolar liquids, respectively.<sup>9</sup> This type of nonattractive behavior increases with the degree of fluorine substitution at each carbon center (i.e.  $\text{CF}_3 > \text{CF}_2 > \text{CF}$ ), and also depends on perfluoroalkyl chain length (greater withdrawal of electron density away from the terminal  $\text{CF}_3$  group occurs up to a value of  $n \approx 7$  for  $\text{CF}_3(\text{CF}_2)_n-$ ).<sup>10,11</sup> It is on this basis that short perfluoroalkyl chains give rise to hydrophobicity, while longer perfluorinated chain lengths are necessary for additional oleophobic behavior. In the latter case, pack-

ing efficiency can become sufficient so as to effectively leave just a layer of  $\text{CF}_3$  groups exposed at the air-solid interface.<sup>12,13</sup> Conventional fluoropolymer coating methods for imparting such oil and water repellency are typically aqueous/organic solvent based.<sup>14,15</sup> They usually contain combinations of resins, catalysts, homo- and copolymers, surfactants, pH adjusters, and cross-linking agents and require heat to effect fixation, etc.<sup>16-18</sup> Examples include polymers, copolymers,<sup>19-21</sup> and cross-linked structures with fluorinated side chains.<sup>22</sup> Surface energy values well below the  $18.5 \text{ mN m}^{-1}$  for polytetrafluoroethylene (PTFE)<sup>8</sup> have been reported for these systems.

An alternative solventless approach is to deposit liquid-repellent perfluoroalkyl chains onto solid surfaces by plasma polymerization.<sup>24</sup> Such "cold" plasmas contain heavy particles (gas atoms, molecules, radicals, and ions) at ambient temperature, photons, and "hot" electrons possessing sufficient kinetic energy to cause bond rupture and further ionization (thereby sustaining the discharge). The passage of pure organic vapor through

- (12) Hare, E. F.; Shafrazi, E. G.; Zisman, W. A. *J. Phys. Chem.* 1954, 58, 236.
- (13) Pittman, A. G.; Sharp, D. L.; Ludwig, B. A. *J. Polym. Sci. Part A-1* 1968, 6, 1729.
- (14) Shimizu, T. In *Modern Fluoropolymers*; Scheirs, J., Ed.; John Wiley and Sons Ltd.: New York, 1997; p 513.
- (15) Thunemann, A. F.; Lieske, A.; Paulke, B. *R. Adv. Mater.* 1999, 11, 321.
- (16) Park, I. J.; Lee, S. B.; Choi, C. K.; Kim, K. J. *J. Colloid Interface Sci.* 1996, 181, 294.
- (17) Tamura, M.; Funaki, H. *JP Patent* 302, 335, 1997.
- (18) Wakida, T.; Tokano, S.; Niiz, S.; Ueda, M.; Mizushima, H.; Takekoshi, S. *Patent Res. J.* 1994, 54, 316.
- (19) Chapman, T. M.; Benashid, R.; Marra, K. G.; Keener, J. P. *Macromolecules* 1996, 29, 331.
- (20) Hopger, J.; Moeller, M. *Macromolecules* 1992, 25, 1461.
- (21) Thomas, R. P.; Anton, D. R.; Graham, W. F.; Darmen, M. J.; Sauer, E. B.; Saka, H. M.; Swartzfager, D. J. *Macromolecules* 1997, 30, 1883.
- (22) Marra, K. G.; Hopger, M. *J. Appl. Polym. Sci.* 1993, 47, 241.
- (23) Sigmund, D. L.; Dobson, C. E.; DeHaven, B. M.; Potter, G. E.; Meyers, S. F.; Fischer, D. A. *Nature* 1994, 368, 39.
- (24) Coulson, S. R.; Brewer, S.; Willis, C.; Badyal, J. P. S. *EP Patent* 0118334, 1997.

this type of medium can lead to the deposition of polymeric films, although structural rearrangement can be a major limitation.<sup>25</sup> Pulsing the electrical discharge on the microsecond-millisecond time scale overcomes this drawback by minimizing damage to the growing polymer layer and enabling conventional polymerization reaction pathways to proceed during the duty cycle off-period.<sup>26</sup> In this study, 1H,1H,2H,2H-heptadecafluorodecyl acrylate ( $\text{H}_2\text{C}=\text{CHCO}_2\text{CH}_2\text{CH}_2(\text{CF}_2)_7\text{CF}_3$ ) has been chosen as the feed monomer. This molecule contains the long perfluorinated alkyl chain needed for liquid repellency and a terminal acrylate group capable of undergoing conventional polymerization<sup>27,28</sup> during the pulsed plasma off-period. Only continuous wave plasma polymerization of fluoroacrylates<sup>29-32</sup> and pulsed plasma deposition of short chain fluoromonomers<sup>33,34</sup> have been previously investigated. These were reported to exhibit limited liquid repellency (typically repelling water and high surface tension alkanes<sup>30</sup>).

## 2. Experimental Section

Plasma polymerization experiments were carried out in an inductively coupled cylindrical glow discharge reactor (5 cm diameter, 470 cm<sup>3</sup> volume, base pressure of  $6 \times 10^{-3}$  mbar, and a leak rate<sup>35</sup> of better than  $6 \times 10^{-9}$  mol s<sup>-1</sup>). This was connected to a two stage Edwards rotary pump via a liquid nitrogen cold trap, a thermocouple pressure gauge, and a monomer tube containing the 1H,1H,2H,2H-heptadecafluorodecyl acrylate monomer (Fluorochem, 98% purity, further purified using multiple freeze-thaw cycles). All connections were grease free. An L-C matching unit was used to minimize the standing wave ratio (SWR) of the transmitted power between a 13.56 MHz radio frequency (RF) generator and the electrical discharge. For pulsed plasma deposition experiments, the RF source was triggered by a signal generator, and an oscilloscope was used to monitor the pulse width and amplitude. The average power ( $P$ ) delivered to the system was calculated using the following formula:<sup>36</sup>

$$\langle P \rangle = P_p [t_{on}/(t_{on} + t_{off})]$$

where  $t_{on}/(t_{on} + t_{off})$  is defined as the duty cycle, and  $P_p$  is the continuous wave power. A typical experimental run comprised initially scrubbing the reactor with detergent and rinsing with isopropyl alcohol, followed by oven drying. The system was then reassembled and cleaned further with a 50 W air plasma for 30 min. Next, the chamber was vented to air, and the

(25) Yasuda, H. *Plasma Polymerization*; Academic Press: Orlando, FL, 1985.

(26) Ryan, M. E.; Hynes, A. M.; Badyal, J. P. S. *Chem Mater.* 1996, 8, 37.

(27) Vohrer, U.; Muller, M.; Oehr, C. *Surf. Coat. Technol.* 1998, 12, 1123.

(28) Hatada, K.; Kobayashi, H.; Masuda, Y.; Kitano, Y. *Polym. Sci. Rep.* 1981, 38, 615.

(29) Morita, S.; Ikeda, S.; Ishibashi, S.; Ieda, M.; Nomatsu, T.; Tamanaka, C. *Int. Symp. Plasma Chem.* 1981, 5, 272.

(30) Chen, W.; Faddeev, A. T.; Hsieh, C.; Oner, D.; Youngblood, J.; McCarthy, T. J. *Langmuir* 1999, 15, 3395.

(31) Shaw, D. G.; Langlois, M. G. *Society of Vacuum Coaters 38th Annual Technical Conference Proceedings*; Society of Vacuum Coaters: Albuquerque, NM, 1995, p 417.

(32) Morita, S.; Yoneza, H.; Ikeda, S.; Ishibashi, S.; Tamanaka, C.; Yamada, Y.; Hattori, S.; Ieda, M. *Int. Symp. Plasma Chem.* 1981, 5, 259.

(33) Lapede, J. B.; Coulson, M. H. *J. Appl. Polym. Sci.* 1999, 74, 1429.

(34) Wang, J. H.; Chen, J. J.; Timmons, R. B. *Surf. Coat. Technol.* 1996, 10, 12.

(35) Eastlich, C. D.; Basford, J. A. *J. Vac. Sci. Technol.* 1992, A10, 1.

(36) Coulson, M. H.; Lapede, J. B. *J. Appl. Polym. Sci.* 1999, 74, 1429.

substrate to be coated was placed into the center of the reactor, followed by evacuation back down to the base pressure. 1H,1H,2H,2H-Heptadecafluorodecyl acrylate vapor was then introduced at a constant pressure of  $\sim 0.1$  mbar and allowed to purge through the system for 5 min, followed by ignition of the glow discharge. Deposition was terminated after 5 min, and the monomer vapor was allowed to continue to pass over the substrate for a further 5 min; subsequently the plasma chamber was evacuated back down to the base pressure and then vented to the atmosphere. The optimum pulsing conditions were arrived at using factorial experimental design, followed by simplex optimization.

Deposition rate measurements were carried out using a gold coated quartz crystal monitor (Inficon KTM/2) located in the center of the reaction chamber.<sup>37</sup> A control experiment where the monomer vapor was allowed to pass over the substrate for 15 min in the absence of the electrical discharge indicated no deposition. Corresponding film thickness values were obtained using a Nanoptix 1kd-6000 scanning spectrophotometer.

Conventional solution phase polymerization of 1H,1H,2H,2H-heptadecafluorodecyl acrylate comprised placing some uninhibited monomer into a round-bottom flask followed by deoxygenation using a stream of argon. Next, lauroyl peroxide dissolved in toluene solution was added to the monomer, followed by flushing the reaction vessel with argon gas to remove the toluene. The reaction mixture was stirred and warmed to 70 °C under a positive flow of argon for 3–4 h. The solid polymer product was then cooled, dissolved in hexafluoropropene, and precipitated into methanol. Excess solvent was decanted off the gelatinous polymer. Further purification was achieved by agitation in hot methanol followed by decanting. Finally, the polymer was dried in a vacuum oven at 25 °C to yield a hard white solid.

A VG ESCALAB MKII electron spectrometer fitted with a nonmonochromated Mg Ka X-ray source (1253.6 eV) and a hemispherical analyzer operating in the CAE mode (20 eV pass energy) was used for X-ray photoelectron spectroscopy (XPS) analysis of the deposited plasma polymer coatings. The photoemitted atomic core level electrons were collected at a takeoff angle of 30° from the substrate normal, which corresponds to a sampling depth of approximately 10–15 Å for the C(1s) envelope.<sup>38</sup> XPS peaks were fitted using a Marquardt minimization computer program assuming linear background subtraction. Elemental concentrations were calculated using instrument sensitivity factors determined from chemical standards, C(1s):O(1s):F(1s) = 1.00:0.36:0.23, respectively. During a typical XPS scan, X-ray beam damage caused less than 1% variation in the F:C ratio; this was sufficiently small that no discernible change was observable in the C(1s) envelope. Complete plasma polymer coverage of the underlying glass substrate was confirmed by the absence of any Si(2p) XPS signal showing through.

A FTIR Mattson Polaris instrument fitted with a Golden Gate single reflection diamond ATR apparatus (Graseby Specac) was used for infrared analysis. Plasma polymerization depositions were carried out onto sodium chloride plates and analyzed using 128 scans at a resolution of 4 cm<sup>-1</sup>.

A Digital Instruments Nanoscope III atomic force microscope was used to examine the physical structure of the plasma polymer coatings deposited onto flat glass substrates. The microscope was operated in Tapping Mode, where changes in the oscillation amplitude of the cantilever tip provide a feedback signal for measuring variations in surface topography. All of the AFM images were acquired in air and are presented as unfiltered data. Root-mean-square RMS roughness values were obtained from 10  $\mu\text{m} \times 10 \mu\text{m}$  images.<sup>39</sup>

(37) Britte, J. J. *Surf. Coat. Technol.* 1985, 57, 105.

(38) Britte, J. J.; Seam, M. P. *Structure Analysis by Auger and X-ray Photoelectron Spectroscopy*; John Wiley and Sons: Chichester, 1991.

(39) AFM 2-4-L14 STOMAF<sup>®</sup> atomic force microscopy system for measuring surface roughness.

## Ultralow Surface Energy Plasma Polymer Films

Table 1. Surface Energies of Probe Liquids

repellency	liquid	surface energy <sup>43</sup> (mN m <sup>-1</sup> at 20 °C)
hydrophobicity	water	72.3
	isopropyl alcohol	21.3
oleophobicity	dodecane	25.4
	octane	21.5
heptane	heptane	20.1
	hexane	18.4
	pentane	16.1

Sessile drop contact angle measurements were carried out at 20 °C using a video capture apparatus (A. S. T. Products VCA2500XE). The Wilhelmy plate technique (Cahn microbalance, Model DCA322) was employed for dynamic contact angle analysis.<sup>40</sup> In this case, a glass slide coated on both sides was suspended from the microbalance, while a motorized stage moved a beaker containing the probe liquid upward and over the substrate at a speed of 154  $\mu\text{m s}^{-1}$ . The advancing contact angle,  $\theta$ , corresponds to the tangent at the three-phase solid–liquid–vapor interface formed during the initial immersion of the plate; this was calculated by applying the modified Young equation:<sup>41</sup>

$$\cos \theta = F/\gamma p$$

where  $F$  is the wetting force at the meniscus measured by the microbalance,  $\gamma$  is the surface tension of the probe liquid, and  $p$  is the perimeter of the meniscus formed at the three-phase interface. The obtained value of  $\theta$  was used to calculate the surface energy (also referred to as surface tension with the corresponding units  $\text{mJ m}^{-2}$  and  $\text{mN m}^{-1}$  being dimensionally equivalent) using two different methods. First, the combined geometric mean Young's equation was used:<sup>41</sup>

$$(1 - \cos \theta)\gamma_i = 2((\gamma_i^d \gamma_i^p)^{1/2} + (\gamma_i^p \gamma_i^d)^{1/2})$$

where  $\gamma_i$  is the surface tension of the probe liquid, and  $\gamma_i^d$  and  $\gamma_i^p$  are the respective dispersive and polar (hydrogen bonding and dipolar–dipolar<sup>42</sup>) components.<sup>43</sup> The dispersive ( $\gamma_i^d$ ) and polar ( $\gamma_i^p$ ) surface energy components for the coating could be calculated by substituting values for water<sup>43</sup> (representative polar liquid,  $\gamma_i^d = 22.1 \text{ mN m}^{-1}$  and  $\gamma_i^p = 50.7 \text{ mN m}^{-1}$ ) and octane<sup>43</sup> (representative nonpolar liquid,  $\gamma_i^d = 21.6 \text{ mN m}^{-1}$  and  $\gamma_i^p = 0.0 \text{ mN m}^{-1}$ ) into the equation and solving the corresponding set of simultaneous equations. Summation of  $\gamma_i^d$  and  $\gamma_i^p$  gave the total surface energy,  $\gamma$ . The alternative approach was to construct a Zisman plot.<sup>3</sup> This comprises choosing a set of probe liquids from the same homologous series (pentane, hexane, heptane, octane, and dodecane) were employed for the plasma polymer surfaces which exhibited no polar contribution<sup>44–47</sup> and measuring their advancing contact angles using the Wilhelmy plate apparatus. A plot of the cosine of the advancing contact angle versus the liquid surface tension ( $\gamma_i$ ) approximates to a linear relationship called the Zisman plot.<sup>3</sup> By extrapolating the line of best fit to  $\cos \theta = 1$ , the critical surface tension of spreading for the solid surface,  $\gamma_s$ , is obtained. Any liquid with a surface tension smaller than this value forms a zero contact angle with the coating. The Wilhelmy plate apparatus was also used to check that the

<sup>40</sup> Andrade, J. D. In *Surface and Interfacial Aspects of Biomedical Polymers*; Andrade, J. D., Ed.; Plenum Press: New York, 1995; Vol. 1, Chapter 7.

<sup>41</sup> Mital, K. L. Ed. *Contact Angle, Wettability and Adhesion*; VSP: B.V. Delft, The Netherlands, 1993.

<sup>42</sup> Fowkes, F. M. *Ind. Eng. Chem.* 1964, 56, 40.

<sup>43</sup> Jaster, J. J. *J. Phys. Chem. Ref. Data* 1972, 1, 541.

<sup>44</sup> Daal, E. N. *Langmuir* 1987, 3, 1103.

<sup>45</sup> Bakkes, A. R. *Van de Sande, H. J. A. P., Willink, P. J.* *Langmuir* 1998, 14, 5807.

<sup>46</sup> Cherry, B. N. *Cambridge Solid State Science Report Series*; Cambridge University Press: Cambridge, England, 1993; p 16.

<sup>47</sup> Kneale, C. H. *J. Adhes.* 1970, 1, 62.

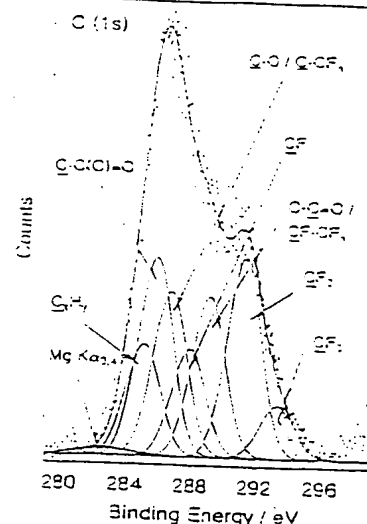


Figure 1. C(1s) XPS spectrum of a 5 W continuous wave plasma polymerized LH<sub>2</sub>H<sub>2</sub>H<sub>2</sub>H-heptadecyltrifluorooctyl acrylate deposited onto a flat glass substrate.

Table 2. Compilation of the Theoretical (Corresponding to the Monomer Structure,  $\text{CH}_2=\text{CHCO}_2\text{CH}_2\text{CH}_2\text{C}_6\text{F}_{13}\text{S}$ ) and Actual Chemical Environments Measured by XPS

conditions	F:C ratio	%CF <sub>2</sub>	%CF <sub>3</sub>
theoretical	1.31	53.3	7.7
conventional polymer	1.22 ± 0.02	44.3 ± 0.1	14.1 ± 0.6
optimum pulsed plasma	1.23 ± 0.06	46.7 ± 0.5	14.5 ± 1.3
5 W CW plasma	0.50 ± 0.18	17.2 ± 4.9	3.9 ± 1.4

surface tension of each probe liquid was consistent with reported literature values,<sup>48</sup> Table 1.

### 3. Results

The C(1s) XPS spectra of the plasma polymer layers deposited onto flat glass substrates could be fitted to seven Gaussian Mg Ka<sub>1,2</sub> components with equal full width at half maximum<sup>49–50</sup> C<sub>2</sub>H<sub>2</sub> at 285.0 eV, CCO=O at 285.7 eV, CO/CCF<sub>2</sub> at 286.6 eV, CF at 287.3 eV, OC=O/CCFCF<sub>3</sub> at 289.0 eV, CF<sub>2</sub> at 291.2 eV, and CF<sub>3</sub> at 293.3 eV (corresponding Mg Ka<sub>3,4</sub> satellite peaks were shifted by ~9 eV toward lower binding energy<sup>51</sup>), Figure 1. The oxygenated/hydrogenated carbon centers originate from the acrylate group in the monomer.<sup>15</sup> In the case of continuous wave (CW) plasma polymerization experiments, the whole range of functionalities was found to be present in significant amounts, Figure 1 and Table 2. Decreasing the duty cycle during pulsed plasma polymerization improved >CF<sub>2</sub> group incorporation, eventually becoming close to the the theoretically expected value for complete structural retention of the perfluoroalkyl chain, Figures 2 and 3 and Table 2. Under these conditions, the concentration of CF<sub>3</sub> functionalities present in the C(1s) envelope appears to be greater than predicted by the monomer structure, Table 2; this is most likely due to the surface sensitivity of the XPS technique, yielding a more intense signal from the

<sup>48</sup> Evans, J. P.; Gibbs, J. H.; Moulder, J. F.; Hammond, J. S.; Pritchard, H. *Practical X-ray Photoelectron Spectroscopy*; Plenum: New York, 1992.

<sup>49</sup> Evans, J. P.; Gibbs, J. H.; Moulder, J. F.; Hammond, J. S.; Pritchard, H. *Practical X-ray Photoelectron Spectroscopy*; Plenum: New York, 1992.

<sup>50</sup> Evans, J. P.; Gibbs, J. H.; Moulder, J. F.; Hammond, J. S.; Pritchard, H. *Practical X-ray Photoelectron Spectroscopy*; Plenum: New York, 1992.

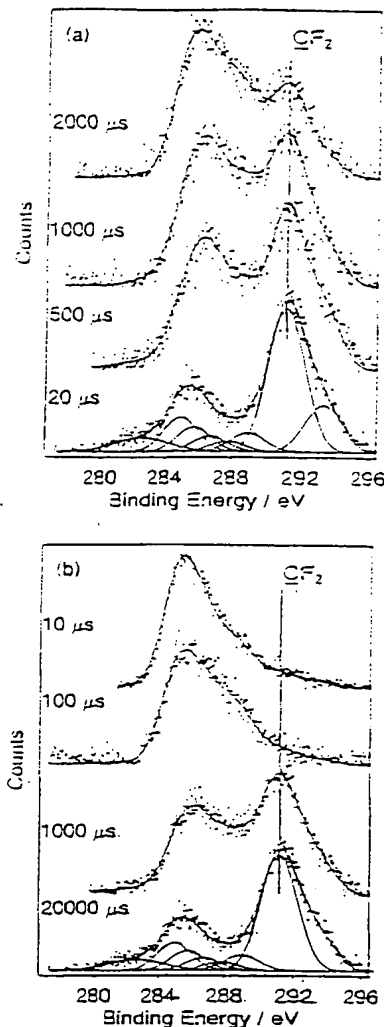


Figure 2. C(1s) XPS spectra of pulsed plasma polymerization of  $1H,1H,2H,2H$ -heptadecafluorododecyl acrylate deposited onto glass with varying (a)  $t_m$  ( $t_m = 20\ 000\ \mu s$ ,  $P_p = 40\ W$ ) and (b)  $t_m$  ( $t_m = 20\ \mu s$ ,  $P_p = 40\ W$ ).

terminal  $\text{CF}_2$  group of the perfluoroalkyl chains aligned away from the coating–substrate interface.<sup>51</sup> The C(1s) signal from ester linkages is consistent with the XPS sampling depth<sup>28</sup> (approximately 1–2 nm), being greater than the length of the perfluoroalkyl side chain.<sup>52</sup> Comparable spectra were obtained for the conventional polymer prepared by solution-phase polymerization of the monomer,<sup>51</sup> Table 2.

Corresponding differences between continuous wave and pulsed plasma deposition were also evident in the infrared spectra, Figure 4 and Table 3. The sharpness of the spectral features associated with the liquid monomer was retained for the pulsed plasma polymer coatings, whereas spectral broadening was evident for continuous wave conditions as a consequence of the higher powers leading to extensive fragmentation, rearrangement, and cross-linking reactions of the parent molecule. Disappearance of the characteristic acrylate carbon–carbon double bond absorption bands at 1640,

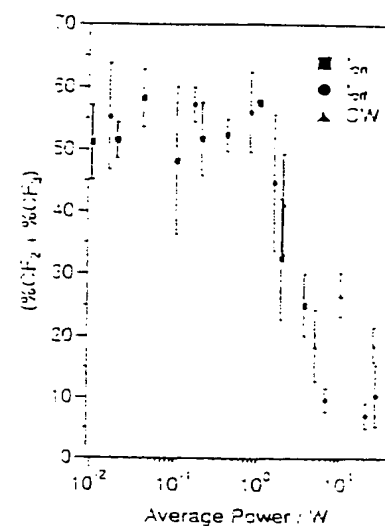


Figure 3. Variation of  $(\% \text{CF}_2 - \% \text{CF}_3)$  concentration versus average power for plasma polymer layers deposited onto flat glass. ( $t_m$  experiments have been carried out at fixed  $t_m = 20\ 000\ \mu s$  and  $P_p = 40\ W$ , while  $t_m$  data corresponds to fixed  $t_m = 20\ \mu s$  and  $P_p = 40\ W$ .)

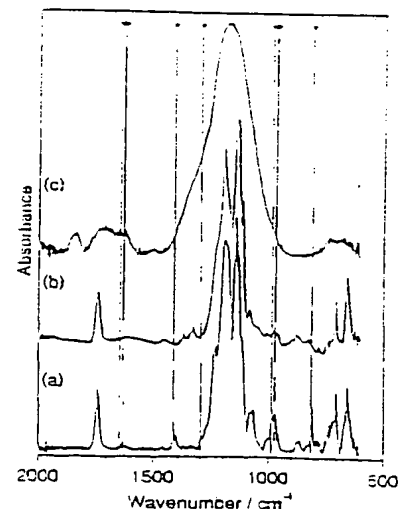


Figure 4. Comparison of infrared spectra: (a)  $1H,1H,2H,2H$ -heptadecafluorododecyl acrylate monomer; (b) pulsed plasma polymerization conditions ( $t_m = 20\ \mu s$ ,  $t_{off} = 20\ 000\ \mu s$ ,  $P_p = 40\ W$ ); and (c) 5 W continuous wave plasma polymerization. NB: \* denotes acrylate carbon–carbon double bond absorption bands.

1625, 1412, 1298, 986, 970, and 812  $\text{cm}^{-1}$  during pulsed plasma polymerization is consistent with reaction proceeding via the acrylate double bond while leaving the associated ester carbonyl group at 1734–1736  $\text{cm}^{-1}$  intact.

The deposition rate was found to pass through a maximum with decreasing average power during pulsed plasma polymerization, Figure 5a. Within this general trend, the observed spread of values for a specific average power indicates the dependency of the polymerization chemistry on the duty cycle parameters, i.e.,  $t_m$  versus  $t_{off}$  period reactions. The optimum pulsed plasma deposition conditions ( $t_m = 20\ \mu s$ ,  $t_{off} = 20\ 000\ \mu s$ ,  $P_p = 40\ W$ ) yielded a film thickness of  $\sim 7\ \mu \text{m}$ .

Atomic force microscopy (AFM) studies gave a RMS roughness value of  $1.7\ \text{nm}$  for the flat glass substrate

<sup>51</sup> Kosec, S.; Shamsi, A.; Shamsi, F.; Iwami, M. *Jpn. J. Appl. Phys.*, **1992**, **31**, 1933.

<sup>52</sup> Jang, J.; Suresh, S.; Tolosa, J.; Gao, J.; Tran, N. T. *Macromol. Chem. Phys.*, **1999**, **200**, 64.

Table 3. Infrared Absorption Band Assignments

group	vibrational mode	Ht. <sup>30</sup>	wavenumber/cm <sup>-1</sup>	
			monomer	pulsed plasma polymer
ester C=O	stretching	1715-1750	1734	1736
acrylate	s-trans and s-cis rotational isomers	1640 and 1625	1640 and 1625	not seen
acrylate	=CH <sub>2</sub> in plane deformation	1410-1420	1412	not seen
-CF <sub>3</sub>	stretching	1120-1050	1117-1236	1117-1196
acrylate	CH in plane deformation	1290-1300	1298	not seen
-CF <sub>2</sub> -	stretching	1120-1230	1117-1236	1117-1196
acrylate	CH out of plane deformation	985-995	986	weak
acrylate	=CH <sub>2</sub> wag	965 ± 5	970	weak
acrylate	=CH <sub>2</sub> twist	311 ± 3	312	not seen

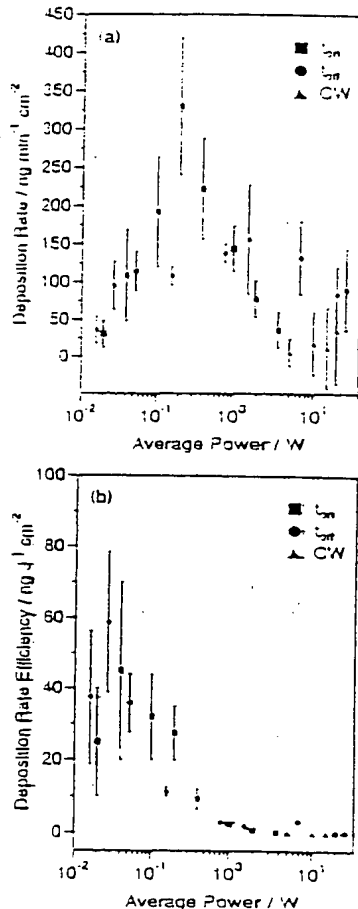


Figure 5. Influence of average power upon (a) deposition rate and (b) deposition rate efficiency. ( $t_{on}$  experiments have been carried out at fixed  $t_{off} = 20\ 000\ \mu s$  and  $P_p = 40\ W$ , while  $t_{on}$  data corresponds to fixed  $t_{on} = 20\ \mu s$  and  $P_p = 40\ W$ .) NB: Nanograms are abbreviated to ng.

and approximately 7 nm for the continuous wave and pulsed plasma polymer films (although their respective morphologies were different), Figure 6. This compares with RMS roughness values of 0.5 nm reported for conventional solution-phase polymerized perfluoroacrylates.<sup>53</sup>

Short-pulse duty cycles gave rise to a drop in surface energy, eventually reaching a limiting value of 10 mN m<sup>-1</sup> as measured by the combined geometric mean Young's equation, Figure 7. Comparison with Figure 3

shows that the polar contribution disappears with increasing structural retention of the perfluoroalkyl chains. The absence of any polar contribution to the total surface energy under these conditions meant that it was valid to use a homologous series of alkane probe liquids to make a Zisman plot; critical surface tension values of  $\gamma_c = 14.4\ mN\ m^{-1}$  and  $\gamma_c = 4.3\ mN\ m^{-1}$  were obtained for continuous wave (5 W) and optimum pulsed ( $t_{on} = 20\ \mu s$ ,  $t_{off} = 20\ 000\ \mu s$ ,  $P_p = 40\ W$ ) plasma polymer coatings respectively, Figure 8. The extremely low critical surface tension value measured in the latter case can be correlated to the observed structural retention of long perfluoroalkyl chains at the air-solid interface. These deposited films were stored in air for over 1 year and showed no sign of aging. This is consistent with the mild nature of pulsed plasma polymerization conditions.

Finally, hydrophobicity and oleophobicity tests were undertaken using a range of pure liquids and water/isopropyl alcohol mixtures with differing surface energies,<sup>27,54</sup> Table 1. This comprised placing 3 drops of each test liquid onto plasma polymer coated cotton fabric. The surface was considered to repel each liquid if, after 30 s, the drops remained spherical/hemispherical, i.e., absence of any penetration or wicking at the liquid-fabric interface. Continuous wave (5 W) plasma deposited coatings were found to be repellent only toward 40%/60% water/isopropyl alcohol mixtures and dodecane (higher concentrations of isopropyl alcohol and shorter alkane chains wetted the substrate). A significant improvement was noted for optimum pulsed plasma deposition conditions, where liquid repellency was observed toward pure isopropyl alcohol as well as water (hydrophobicity), and also alkane chains as short as heptane (oleophobicity), Figure 9. The adhesion of these plasma polymer layers was tested by boil washing in a detergent solution for 15 min followed by drying in an oven at 100 °C. No detachment of the coating from the substrate was observed.

#### 4. Discussion

The described plasma polymerization method is quick, cheap, substrate-independent, and solventless and does not incorporate nonfluorochemical reagents (e.g., catalysts, cross-linking agent, surfactants, etc.,)<sup>14</sup> and therefore a cleaner fluoropolymer product can be expected. The greater retention of  $\text{-CF}_2-$  groups observed during electrically pulsed plasma polymerization compared to continuous wave conditions is consistent with these

<sup>53</sup> Ibrahim, P.; Stoen, M.; Thorpe, A.; Neved, M.; Touboulis, J. *Proceedings of PFA Plastics in Coatings '97*, Teddington, England, 1997; p 1.

<sup>54</sup> 1 CM water repellency test (1 water/water drop test). CM Test Methods, 1986. CM oil repellency test (1 CM Test Methods, Oct 1986).

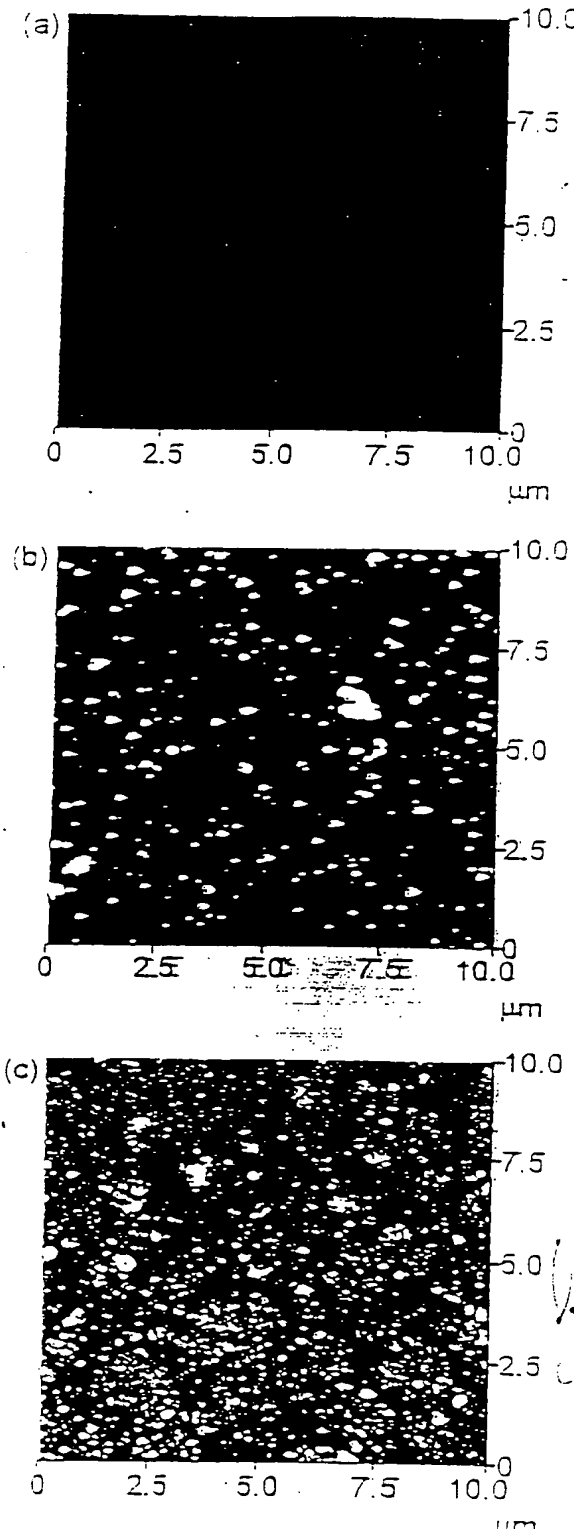


Figure 6. AFM micrographs ( $z = 100$  nm): (a) flat glass substrate; (b) 5 W continuous wave plasma polymer of 1H,1F,2H,2H-heptadecafluorooctadecyl acrylate deposited onto glass; (c) pulsed plasma polymer of 1H,1F,2H,2H-heptadecafluorooctadecyl acrylate deposited onto glass ( $f_{\text{on}} = 20$  Hz,  $t_{\text{off}} = 20\ 000$   $\mu$ s,  $P_p = 40$  W).

fragmentation and damage of the perfluoroalkyl tail. Figure 1 and Table 1. This can be attributed to a drop in plasma sheath potential, causing less energetic ion bombardment of the growing film,<sup>55</sup> as well as attenu-

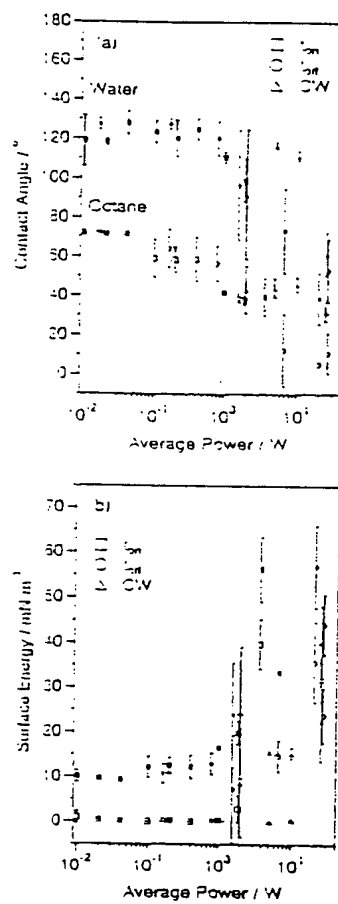


Figure 7. Influence of average power upon (a) water (shaded) and octane (unshaded) advancing contact angles and (b) surface energy values calculated using combined geometric mean Young's equation where the unshaded symbols correspond to the polar component and the shaded ones are the total surface energy.

ation of vacuum-UV irradiation.<sup>56</sup> Good adhesion of the plasma polymer layer occurs due to the creation of free radical sites on the substrate surface during the initial stages of plasma deposition. While the observed difference in film morphology stems from the different mechanistic modes of polymerization (pulsed versus continuous wave).

Normally the deposition rate is found to increase with rising average power for continuous wave conditions.<sup>25</sup> However a reversal in this trend occurred during pulsed plasma polymerization of 1H,1F,2H,2H-heptadecafluorooctadecyl acrylate, Figure 5a. Poor deposition measured at very short duty cycles can be ascribed to the lack of polymerization sites. A maximum is reached at intermediate pulse cycles, corresponding to the highest ratio of polymerizable species to nonpolymerizable/ablative species. Eventually toward continuous wave conditions, the deposition rate drops as a consequence of ablation becoming a competing process. To factor out the effect of variation in average power, the deposition rate efficiency was calculated, defined as deposition rate

<sup>55</sup> Pandalingam, M.; Chen, M.; Hsu, H.; Savage, J. S.; Mumtaz, R. B.; Elford, R. J. *Adv. Polym. Sci.* 1993, 103, 145.  
<sup>56</sup> Yamaoka, H.; Hsu, C. J. *Polym. Sci. Polym. Chem. Ed.* 1977, 15, 11.

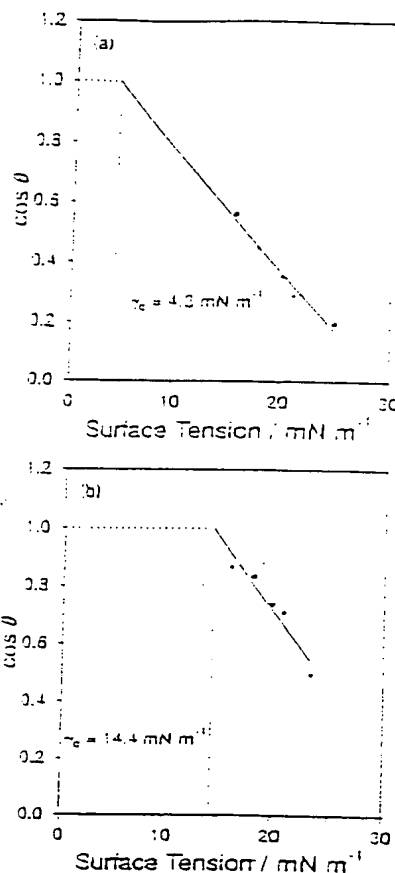


Figure 8. Zisman plot of plasma polymer coated glass slide: (a) pulsed ( $t_p = 20 \mu\text{s}$ ,  $t_m = 20\,000 \mu\text{s}$ ,  $P_p = 40 \text{ W}$ ) and (b) 5 W continuous wave.

divided by average power),<sup>57</sup> Figure 5b. It is found that the deposition rate per joule of energy increases with decreasing average power, which can be taken as being indicative of species which are activated during the on-period (via UV irradiation, ion, or electron bombardment etc.), continuing conventional polymerization either in the gas phase or at the plasma–substrate interface during the off-period of the pulse cycle.<sup>45</sup>

Most previous studies have utilized the Zisman method to assess low surface energy coatings. The critical surface tension values,  $\gamma_c$ , measured for solution phase polymerized  $1H,1H,2H,2H$ -heptadecafluorodecyl acrylate and other long-chain perfluoromonomers and copolymers can be as low as  $3 \text{ mN m}^{-1}$ .<sup>11,12,14,16,51,52,58-63</sup> It appears that the value of  $\gamma_c = 4.3 \text{ mN m}^{-1}$  attained in the present case for the pulsed plasma polymer coatings is comparable. This is particularly surprising since the perfluorocalkyl groups attached to alternate carbon atoms along the polymer backbone should not pack as close together (if this is indeed what actually happens for the pulsed plasma polymer) as fluorocarbon-acid monolayers<sup>13</sup> or epitaxially grown perfluorosilane

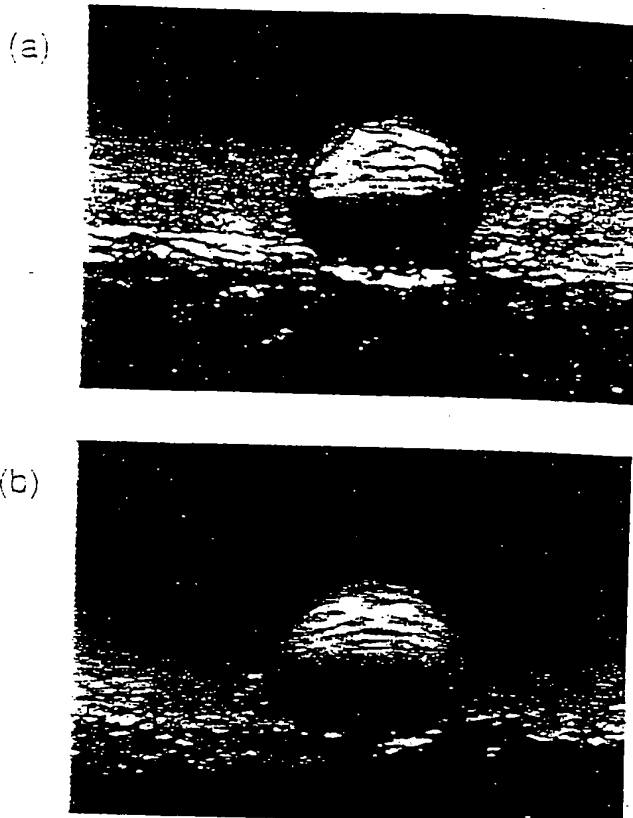


Figure 9. Optical images illustrating liquid repellency ( $2 \mu\text{L}$  droplet volume) for  $1H,1H,2H,2H$ -heptadecafluorodecyl acrylate pulsed plasma polymer layer deposited onto cotton fabric ( $t_p = 20 \mu\text{s}$ ,  $t_m = 20\,000 \mu\text{s}$ ,  $P_p = 40 \text{ W}$ ): (a) pure isopropyl alcohol droplet and (b) heptane droplet.

crystallites,<sup>64,65</sup> for which  $\gamma_c$  values of  $6 \text{ mN m}^{-1}$  have been reported.<sup>9,12,65,66</sup> The microroughness discernible in the AFM micrographs could potentially distort the Zisman plot to give anomalous  $\gamma_c$  values. If the roughness causes air to become trapped in the voids (i.e. the liquid cannot penetrate into the troughs), then a composite interface will be formed in accordance with the Cassie–Baxter relationship<sup>57</sup> (in fact this is how high water repellency has been achieved in the past for powdered plasma polymer films<sup>30,63-71</sup>). However such behavior appears to be unlikely, since the low contact angle hysteresis normally associated with a composite interface<sup>50,72,73</sup> is absent for the pulsed plasma polymer layers (advancing and receding contact angle values,  $\theta_{adv}/\theta_{rec} = 134^\circ/66^\circ$  and  $73^\circ/56^\circ$  for water and octane, respectively). The observed contact angle hysteresis is more consistent with the surface roughness only being

<sup>57</sup> Chen, H.; Rameshwar, K.; Pilkington, P. B.; Green, W. J.; Jayan, M. P. *Surf. Interface Anal.* 1994, 21, 1057.  
<sup>58</sup> Johnson, R. E.; Decra, R. H. *Polym. Prepr. Am. Chem. Soc. Div. Polym. Chem.* 1987, 28, 48.  
<sup>59</sup> Bernini, M. H.; Decra, R. H. *J. Polym. Chem.* 1962, 38, 1927.  
<sup>60</sup> Rameshwar, K.; Jayan, M. P. *J. Polym. Sci.* 1987, 15, 93.  
<sup>61</sup> Jayan, M.; Chandra, A.; Kurihara, S.; Nittoen, Kiyoshi; Matsui, T. *J. Polym. Sci.* 1984, 12, 1145.  
<sup>62</sup> Hotta, T.; Ueda, M. *Macromolecules* 1992, 25, 1461.  
<sup>63</sup> Kurokawa, H. *Macromol. Chem.* 1980, 184, 1589.

<sup>64</sup> Nishino, T. *Proc. Annu. Congr. Adhes. Soc. Jpn.* 1998, 36, 95.  
<sup>65</sup> Nishino, T.; Meguro, M.; Nakamae, T.; Matsushita, M. *Ueca. Langmuir* 1999, 15, 4321.  
<sup>66</sup> Pittman, A. G. In *High Polymers XXV: Fluoropolymers*; Wall, L. A., Ed.; John Wiley and Sons: New York, 1972; Chapter 13.  
<sup>67</sup> Cassie, A. B. D.; Baxter, S. *Trans. Faraday Soc.* 1944, 40, 546.  
<sup>68</sup> Horomi, A.; Sato, J. *Thin Solid Films* 1997, 303, 222.  
<sup>69</sup> Wada, S. D. *Org. Coat. Appl. Polym. Sci. Proc.* 1982, 47, 19.  
<sup>70</sup> Groot, P.; Schneuwly, A.; Schlaepbach, L.; Gaie, M. *J. Vac. Sci. Technol.* 1996, A14, 1043.  
<sup>71</sup> Sato, J.; Wada, M.; Hamamoto, M. *Polym. Prepr. Am. Chem. Soc. Div. Polym. Chem.* 1998, 39, 926.  
<sup>72</sup> Gassan, F.; Morra, M.; Decra, R. *Polymer Surfaces: From Physics to Technology*; John Wiley and Sons: Chichester, England, 1994; p 182.  
<sup>73</sup> Johnson, R. E.; Decra, R. H. *Adv. Chem. Ser.* 1963, 3, 112.

sufficient to produce an effective increase in surface area without pore formation. This can be described in terms of Wenzel's law,<sup>30,53,74</sup> which predicts that surface roughening decreases/increases the repellency of liquids which make a contact angle of less/greater than 90° on the corresponding flat surface. On this basis, any distortion of the critical surface tension value,  $\gamma_c$ , to an abnormally small value as a consequence of surface roughness is also unlikely, since the chosen series of low surface tension alkane probe liquids all exhibit contact angles less than 90°, and according to Wenzel's law,<sup>35,75</sup> surface roughness will actually make the measured liquid contact angle lower than the true value,<sup>75,77,78</sup> hence  $\cos \theta$  will be greater for each probe liquid on the Zisman plot, thereby shifting the  $\gamma_c$  value artificially higher. Hence, the true  $\gamma_c$  value would be expected to be lower than 4.3 mN m<sup>-1</sup>. This may be attributed to atomic fluorine generated via minor fragmentation of some monomer during the duty cycle on-period substi-

tuting hydrogen atoms<sup>79</sup> belonging to the 1H,1H,2H,2H-heptadecafluorodecyl acrylate repeat unit contained in the growing plasma polymer film. For instance, it is well-known that replacement of the hydrogen atom located at the 2-position in the acrylate group with fluorine reduces the critical surface tension of the corresponding solution-phase polymerized product.<sup>14,51</sup>

### 5. Conclusions

Pulsed plasma polymerization is an effective method for the solventless functionalization of solid surfaces. Short duty cycle on-times in conjunction with long off-times enable selective activation of reactive bonds within a monomer. Precursors containing long perfluoroalkyl chains (e.g. 1H,1H,2H,2H-heptadecafluorodecyl acrylate) have been found to yield low surface energy coatings which display no polar contribution and exhibit excellent repellency toward low surface tension liquids.

**Acknowledgment.** S.R.C. would like to thank DERA for a Ph.D. studentship.

CM000193P

(74) Takai, O.; Hozumi, A.; Inoue, Y.; Komori, T. *Bull Mater. Sci.* 1997, 20, 317.  
 (75) Wenzel, R. N. *Ind. Eng. Chem.* 1936, 28, 388.  
 (76) Wenzel, R. N. *J. Phys. Chem.* 1949, 53, 1466.  
 (77) Moillet, J. L. *Water Proofing and Water Repellency*; Elsevier: London, 1963; p 28.  
 (78) Drelich, J.; Miller, J. D.; Good, R. J. *J. Colloid Interface Sci.* 1996, 179, 37.

(79) Cain, S. R.; Egito, F. D.; Emani, F. J. *J. Vac. Sci. Technol.* 1987, A5, 1578.